

Fano Resonance and Electron Filtering in Multiply-Connected Carbon Nanotubes

Gunn Kim,¹ Sang Bong Lee,¹ Tae-Suk Kim,¹ and Jisoon Ihm^{1,*}

¹*School of Physics, Seoul National University, Seoul 151-747, Korea*

(Dated: July 20, 2022)

We investigate the electron transport in multiply-connected metallic carbon nanotubes within the Landauer-Büttiker formalism. Quasibound states are coupled to the incident π^* states and give rise to energy levels of different widths depending on the coupling strength. In particular, donor-like states originated from heptagonal rings are found to give a very narrow level. Interference between broad and narrow levels produces Fano-type resonant backscattering as well as resonant tunneling. Over a significantly wide energy range, almost perfect suppression of the conduction of π^* electrons occurs, which may be regarded as filtering of particular (π^*) electrons.

PACS numbers: 73.23.-b, 73.61.Wp, 73.63.Fg

In the past decade, carbon nanotubes (CNTs) have been studied extensively because of their unconventional properties from both the fundamental research and application point of view [1, 2]. For the application to nanoscale electronic devices, researchers have fabricated various forms of CNTs to engineer their physical properties [3, 4, 5]. Recently, novel morphologies such as X- and T-shaped junctions have been produced by electron beam irradiation at high temperature in a high-resolution transmission electron microscope [6]. There is considerable evidence that transport through finite-sized CNT devices occurs via resonant transmission [7, 8], and the phase coherence of electron's wavefunction can be observed in mesoscopic systems. A typical manifestation of the phase coherence is the Fano resonance which arises from the coherent interference between a narrow localized level and a continuum energy spectrum [9]. The Fano effect has been very actively studied in the nanoscale devices recently. It was observed in the conductance when the quantum dot was embedded into one arm of the Aharonov-Bohm interferometer [10]. It was also identified in the direct transport through a single quantum dot [11, 12]. This effect still remains to be explored in the finite-sized CNT devices.

In this Letter, we report novel transport properties in a multiply-connected carbon nanotube (MCCN) structure as shown in Fig. 1, where a single tube is branched off into two smaller arms and then they merge into one. We have studied conductance variation systematically by changing the length of the arms. Both π -bonding and π^* (π anti)-bonding electron transport channels are featured with the resonant tunneling through the discrete energy levels (DELs) in the finite arms of (5,5) tubes. The width of the resonant tunneling peaks in the π channel is broad and the transmission probability is fairly uniform as a function of energy. The π^* channel, on the other hand, has more interesting structure of either broad or narrow resonant tunneling. Coherent interference between a very broad peak (extending over to nearby peaks) and its narrow neighboring peak is evident in the asymmetric Fano-type lineshapes of the π^* transport channel

and the corresponding transmission probability is featured with both zero and one. In particular, we find a nearly perfect suppression of the π^* transmission in a certain finite range of energy. This mechanism can be regarded as electron filtering of a particular (π^*) wavefunction character, and such a nonequilibrium distribution may be maintained over the relaxation length of the electron phase beyond the arm region.

Our model system, the MCCN, comprises two leads of semi-infinite metallic (10,10) CNTs and two arms of finite (5,5) tubes (effectively a resistive region) in between. This structure may be thought as two Y-junctions faced to each other, possibly produced experimentally by electron irradiation on nanotubes. Six heptagons are contained in each of two junction regions where the (10,10) tube and two (5,5) tubes are joined. Six heptagons near each junction area act as an effective potential barrier for electrons incident from the lead of the (10,10) tube. The length of the arm region is represented by the number (L) of periodic units of the armchair CNT as shown in Fig. 1. This structure possesses the mirror symmetry with respect to three planes. Two symmetry planes σ_p and σ_c , which are, respectively, perpendicular to and containing the (10,10) tube axis, are indicated in Fig. 1. The third one is the plane of the figure containing the

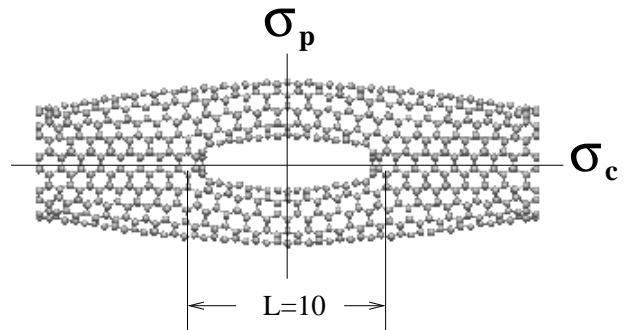


FIG. 1: Model of MCCN with $L=10$. σ_p and σ_c denote the planes of mirror symmetry.

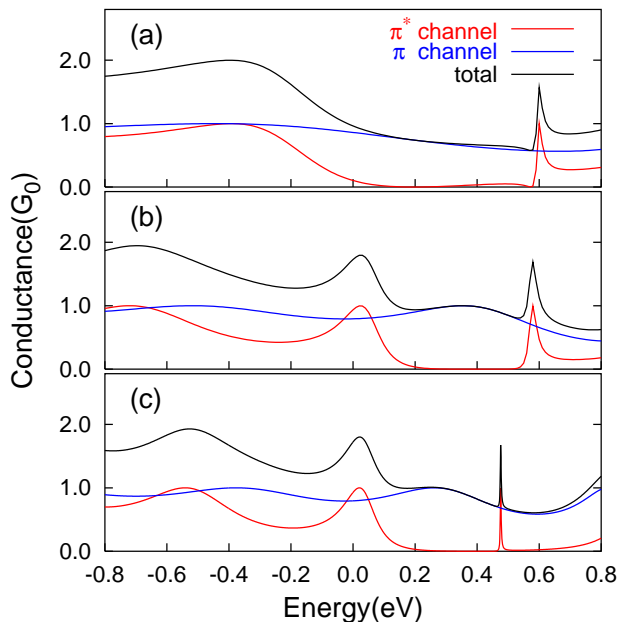


FIG. 2: (color online). Conductance as a function of the incident energy E for the MCCNs. The Fermi level is set to zero. (a) $L=5$, (b) $L=9$, and (c) $L=12$.

tube axis (not indicated in Fig. 1). The electronic structure is described by the single π -electron tight-binding Hamiltonian with the nearest-neighbor hopping integral $V_{pp\pi} = -2.66$ eV [13].

The π and π^* bands are crossing at the Fermi energy (E_F) in the armchair CNTs and only these two bands contribute to the electron transport if the bias voltage is not large. The π and π^* transport channels are usually admixed when defects are introduced into the perfectly periodic nanotubes. However, the two transport channels remain unmixed in our MCCN because of the σ_c symmetry of the structure. We compute the transmission coefficients of electron waves incident to the resistive region from one of the leads. Conductance is obtained from the Landauer-Büttiker formula, $G(E) = G_0 \text{Tr}(\mathbf{t}^\dagger \mathbf{t})$, where G_0 is the conductance quantum ($= 2e^2/h$) and \mathbf{t} is the transmission matrix [14, 15].

The conductance as a function of the incident electron energy is displayed in Fig. 2 for the cases of $L = 5, 9$ and 12 . To examine the structure of the conductance in detail, total conductance is decomposed into two nonmixing contributions of π and π^* channels, $G = G_0(T_\pi + T_{\pi^*})$, where T_π and T_{π^*} are the transmission probabilities of the two. We find the following features common to various L 's. (i) T_π has peaks of magnitude one always and varies very slowly in energy. (ii) T_{π^*} has both broad and narrow peaks of magnitude one always, and the lineshape is highly asymmetric, especially for narrow peaks. (iii) T_π has no zeros within the interested energy window while T_{π^*} is featured with zeros near the narrow asymmetric peaks.

Since the wavefunctions of π states do not have phase variation in the circumferential direction (i.e., over the cross-section of the tube) irrespective of n in (n,n) tubes, π wavefunctions in the lead parts ((10,10) tubes) have almost perfect match with those in the arms ((5,5) tubes), and the transmission is close to one in a wide range of energy. On the other hand, the conduction of π^* electrons is more complicated and may be explained by a close examination of the resonant tunneling through the DELs which are accommodated in the arms of (5,5) tubes. Considering the energy quantization by confinement to a finite region, we expect with increasing length L of (5,5) tubes that the spacing between peaks becomes smaller. Peaks for the π^* states in Fig. 2 show this trend unambiguously. (Needless to say, π electrons also experience resonant tunneling via DELs as exemplified in the series of peaks of magnitude one. However, their linewidth is so broad that the variation in the conductance is small and uninteresting.) The spectrum of DELs can be roughly estimated from the linear dispersion [16] near E_F for the ideal armchair nanotube,

$$|E(k)| = \frac{a\sqrt{3}}{2} |V_{pp\pi}| |k - k_F|, \quad (1)$$

where a ($= 2.46$ Å) is the lattice constant and k_F ($= 2\pi/3a$) is the Fermi wave vector. Approximate values of the spectrum of DELs are found from the quantization condition $kd = m\pi$, where d is the effective length of the arm and m is positive integer. For instance, if we took $d = La$ ($L = 13$) for $k = m\pi/d$, the DELs near E_F would be $-0.93, -0.37, 0.19,$ and 0.74 eV. A better fitting to the exact numerical calculation in Fig. 3(a) could be obtained if we assumed a longer effective length $d \approx (L + 1.5)a$, in which case we would have $-0.82, -0.32, 0.18,$ and 0.68 eV. This result is reasonable since the electrons localized in the central ring region are somewhat spread out beyond the arms as seen, for instance, in the last picture of Fig. 3(b). This simple model based on the linear dispersion, of course, has a limitation of obtaining, incorrectly, the same energy separations only.

Coupling to the left and right semi-infinite metallic tubes results in the finite lifetime (line broadening) of the DELs. To understand the variation of the linewidth from peak to peak, we further investigate the structure of the wavefunctions at the resonant peaks. Besides the linear π and π^* bands crossing at E_F , there exist a conduction band at 0.8 eV and above, and a valence band at -0.8 eV and below in the (10,10) tube. Because of the presence of the heptagonal carbon rings at the junction, donor-like states tend to be produced according to well-known Hückel's $(4n + 2)$ rule for stability [17]. The cycloheptatrienyl cation is a molecular example of the heptagonal ring following Hückel's rule for $n = 1$. The localized impurity (donor) state is most pronounced if the energy level is close to (and below) aforementioned conduction band minimum at 0.8 eV. Such localized donor-

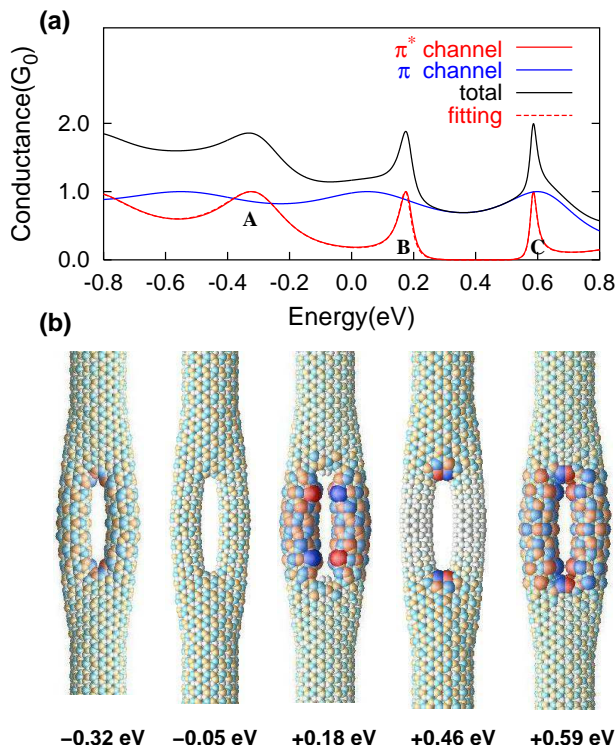


FIG. 3: (color online). Conductance and wavefunctions for $L=13$. In (a), the full numerical calculation for π^* (solid red line) is indistinguishable from the fit with the multiple Fano resonance formula (red dashed line). In (b), the red and blue colors indicate \pm signs and the size of the spheres is the amplitude of the wavefunction.

like states have in fact been found in other defects (nitrogen impurity and Stone-Wales defect) of the nanotube as well [18, 19]. The peak C in Fig. 3 (or sharp peaks closest to 0.8 eV in Fig. 2) corresponds to this state and has a narrow lineshape owing to the relatively well-localized (long lifetime) character of such an origin. The DELs further away from the conduction band minimum are less localized and thus broader.

We also compare the wavefunctions around the peaks and the nodes of the conductance curve. The wavefunctions at peaks of T_{π^*} have large amplitude in two arms so that incident electrons are in resonance with the states in the region. In contrast, the wavefunctions of the π^* band at the U-shaped valley (e.g., at 0.46 eV in Fig. 3(b)) are depleted inside two arms, which means an effective disconnection of two leads and the suppression of the electron conduction. Unlike in the π electron case, the phase variation of the cross-section of the tube is very rapid in the π^* state and it is very difficult to match the wavefunction at the junction boundary for a general value of energy, hence substantial reduction in conductance.

So far, we have explained the interesting phenomenon of linewidth variations from level to level. Such a variation leads to even more profound consequences on the structure of the transmission probability as we shall de-

scribe below. In the 1D mesoscopic systems such as the double-barrier quantum wells, if all the DELs are coupled to the continuum of lead states with almost the same constant coupling strength and the relative signs of couplings to two leads are alternating from level to level, the transmission zero does not occur [20]. However, when one energy level is coupled by far more strongly to the leads and acts like a broad band interfering with other narrow levels, the transmission zero may take place [20]. Our system falls in the latter case. As the energy of the DELs is increased, the number of nodes along the two arms increases one by one and in turn the relative signs of the wavefunctions at two junctions are oscillating for DELs. This alternating parity under σ_p symmetry operation is clearly visible in Fig. 3(b) for DELs at -0.32 (even), 0.18 (odd), and 0.59 eV (even). In the presence of the σ_p symmetry (plus the time-reversal symmetry which obviously exists in the absence of applied magnetic fields), it is well known that the perfect transmission ($T_{\pi^*} = 1$) is allowed to occur at all resonant peaks in the system [21]. On the other hand, the transmission zero is generally not allowed in the energy range between one level and its nearest neighbor level interfering each other [20]. It is only when a broad level extends beyond the nearest neighbor narrow level that a transmission zero occurs at the energy between its nearest and *next nearest neighbor* narrow level.

To confirm this argument, we fit the curve of T_{π^*} for $L = 13$ with the multilevel formula. The expression for T contains, as parameters, discrete energy levels E_i and coupling constants with right (V_{Ri}) and left leads (V_{Li}) [20].

$$T(\epsilon) = 4\text{Tr}\{\Gamma_L D^r(\epsilon) \Gamma_R D^a(\epsilon)\}, \quad (2)$$

$$D^{r,a}(\epsilon) = [\epsilon I - E \pm i\Gamma]^{-1}, \quad (3)$$

where $E_{ij} = E_i \delta_{ij}$, $\Gamma_{ij} = \Gamma_{Lij} + \Gamma_{Rij} = \pi N_L V_{iL} V_{Lj} + \pi N_R V_{iR} V_{Rj}$ and $N_{L,R}$ is the density of states. We use seven DELs and their diagonal components of Γ ($V_{Ri} = \pm V_{Li}$, $N_L = N_R$). Values of DELs (Γ_{ii}) in eV are as follows: $-1.330(0.139)$, $-0.859(0.194)$, $-0.300(0.132)$, $0.178(0.025)$, $0.584(0.013)$, $1.100(0.183)$, and $1.700(0.250)$. The conductance curve in much wider energy range than the one presented in Fig. 3 has been fitted for more complete results. As mentioned above, relative signs of the wavefunction at two junctions alternate from one level to the next. Therefore, between peaks A and B (i.e., the right-hand side of A and left-hand side of B), two conduction paths interfere constructively and no transmission zero occurs. However, on the right-hand side of B, A and B interfere destructively (since the energy is greater than both A and B) and produce a transmission zero. This is possible because peak A is so broad that its tail extends substantially over to the right-hand side of B. Since peak C is very narrow, its constructive

interference on B (in the energy range between B and C) is much less than the destructive interference from A and unable to change the result. In fact, there are two transmission zeros between B and C, one nearer to B which is obtained as above and the other nearer to C which is obtained by the destructive interference between C and the next broad peak above C (not shown). The curve fitting with Eq. (2) is practically perfect and indistinguishable from the full numerical calculation in the energy range we have studied, indicating that the multilevel transmission formula of the type in Eq. (2) and (3) is indeed valid. We also note that, in a certain finite energy range, the conductance of π^* electrons is almost zero while that of π electrons is not reduced appreciably. For instance, the transmitted electrons of π^* character for $L = 5$ in Fig. 2(a) constitute less than 8% of the total transmitted electrons in the energy range between 0 and 0.5 eV. This may be regarded as electron filtering of a particular (π^*) wavefunction character. Such a nonequilibrium distribution persists over the relaxation length of the electron phase beyond the arm region. This result can be used for a further fundamental research on the electronic character in nanostructures or an application to current switching in nanotubes.

In summary, we have performed tight-binding calculations of conductance of multiply-connected metallic CNTs with the mirror symmetry. The π channel is well-conducting and has very broad resonance peaks. The π^* channel exhibits asymmetric Fano resonance structures. The Fano effect is originated from the interference between broad and narrow electronic levels in the arm region. It is shown that the present system transmits predominantly π over π^* electrons in a certain energy range.

We are grateful to Prof. H.J. Choi for valuable discussions. This work was supported by the CNNC of Sungkyunkwan University, the MOST through the NSTP (grant No. M1-0213-04-0001), the grant No. R01-1999-000-00031-0 from the KOSEF, and the Korea Research Foundation Grant (KRF-2003-C-00038).

-
- * corresponding author. E-mail: jihm@snu.ac.kr
- [1] R. Saito, G. Dresselhaus, and M.S. Dresselhaus, *Physical Properties of Carbon Nanotubes* (Imperial College Press, London, 1998).
 - [2] C. Dekker, Phys. Today **52**(5), 22 (1999).
 - [3] B.W. Smith, M. Monthieux, and D.E. Luzzi, Nature (London) **396**, 323 (1998).
 - [4] K. Hirahara *et al.*, Phys. Rev. Lett. **85**, 5384 (2000).
 - [5] A.N. Andriotis, M. Menon, D. Srivastava, and L. Chernozatonskii, Phys. Rev. Lett. **87**, 66802 (2001); M. Menon, A.N. Andriotis, D. Srivastava, I. Ponomareva, and L. Chernozatonskii, *ibid.* **91**, 145501 (2003).
 - [6] M. Terrones *et al.*, Phys. Rev. Lett. **89**, 75505 (2002).
 - [7] S.J. Tans *et al.*, Nature (London) **386**, 474 (1997).
 - [8] L.C. Venema *et al.*, Science **283**, 52 (1999).
 - [9] U. Fano, Phys. Rev. **124**, 1866 (1961).
 - [10] K. Kobayashi, H. Aikawa, S. Katsumoto, and Y. Iye, Phys. Rev. Lett. **88**, 256806 (2002).
 - [11] J. Göres, D. Goldhaber-Gordon, S. Heemeyer, M.A. Kastner, H. Shtrikman, D. Mahalu, and U. Meirav, Phys. Rev. B **62**, 2188 (2000).
 - [12] I.G. Zacharia, D. Goldhaber-Gordon, G. Granger, M.A. Kastner, Yu. B. Khavin, H. Shtrikman, D. Mahalu, and U. Meirav, Phys. Rev. B **64**, 155311 (2000).
 - [13] X. Blase, L.X. Benedict, E.L. Shirley, and S.G. Louie, Phys. Rev. Lett. **72**, 1878 (1994).
 - [14] R. Landauer, Philos. Mag. **21**, 863 (1970).
 - [15] M. Büttiker, Phys. Rev. Lett. **57**, 1761 (1986).
 - [16] J.W. Mintmire, D.H. Robertson, and C.T. White, J. Phys. Chem. Solids **54**, 1835 (1993).
 - [17] T.W.G. Solomons, *Organic Chemistry* (Wiley, New York, 1996).
 - [18] H.J. Choi, J. Ihm, S.G. Louie, and M.L. Cohen, Phys. Rev. Lett. **84**, 2917 (2000).
 - [19] H. Kim, J. Lee, S.-J. Kahng, Y.-W. Son, S.B. Lee, C.-K. Lee, J. Ihm, and Y. Kuk, Phys. Rev. Lett. **90**, 216107 (2003).
 - [20] T.-S. Kim and S. Hershfield, Phys. Rev. B **67**, 235330 (2003).
 - [21] H.-W. Lee and C.S. Kim, Phys. Rev. B **63**, 75306 (2001).